Articles

Poly(styrene-*b*-4-vinylphenoxyphthalonitrile)−Cobalt Complexes and Their Conversion to Oxidatively Stable Cobalt Nanoparticles

V. V. Baranauskas III,[†] M. A. Zalich,[†,‡] M. Saunders,[§] T. G. St. Pierre,[‡] and J. S. Riffle*[,†]

Macromolecules and Interfaces Institute, Virginia Polytechnic Institute and State University, Blacksburg, Virginia 24061, and School of Physics and Center for Microscopy and Microanalysis, The University of Western Australia, Crawley, WA 6009, Australia

Received October 13, 2004. Revised Manuscript Received June 22, 2005

Oxidatively stable, magnetic cobalt nanoparticles have been prepared by heating cobalt nanoparticles encapsulated in poly(styrene-*b*-4-vinylphenoxyphthalonitrile) block copolymers at elevated temperatures. The block copolymers were synthesized through the sequential anionic polymerization of styrene and *tert*-butyldimethylsilyloxystyrene. The silyl ether protecting groups on the second block were hydrolyzed under acidic conditions to afford poly(styrene-*b*-4-vinylphenol), and then the pendent phenols of the diblock copolymer were chemically modified with 4-nitrophthalonitrile to afford poly(styrene-*b*-4-vinylphenoxyphthalonitrile). Stable suspensions of ∼8−10 nm diameter cobalt metal nanoparticles were formed by thermolysis of dicobalt octacarbonyl in solutions of toluene containing poly(styrene-*b*-4-vinylphenoxyphthalonitrile). The cobalt−polymer nanoparticle complexes were pyrolyzed under argon to afford highly magnetic cobalt nanoparticles encased in graphitic-like coatings. Magnetic susceptibility measurements indicate that the cobalt−graphitic particles are oxidatively stable and retain their high saturation magnetizations (∼95−100 emu g^{-1}) for at least 1 year under ambient conditions.

Introduction

Magnetic fluids, also referred to as ferrofluids or magnetic colloids, are stable colloidal suspensions of nanometer-size magnetic particles dispersed in a carrier liquid. These materials display typical properties of fluids and behave as intrinsic liquid magnets that move as an entity in the direction of an applied magnetic field gradient.[1] The foundation of magnetic fluid research has been established over many years, and the reader is particularly referred to the work of Hess and Parker,[2] Rosensweig,[3] Smith et al.,[4] and Papirer and Horny.[5] Magnetic fluids have been developed for commercial use in a number of applications including loud speakers, rotating shaft seals, exclusion seals, dampers, and magnetic recording media.[6]

A remarkable amount of promising research focusing on potential applications of magnetic particles has also been published. A number of foreseen applications currently being developed include magnetic field-directed drug targeting,[7] contrast agents for magnetic resonance imaging,[8] gene therapy,[9] and hyperthermia treatment for cancer patients.[10] An area of considerable interest is the use of magnetic particles for separations of biomolecules such as nucleic acids, proteins, and antibodies.[11] Moreover, magnetic particles with covalently linked antibodies may be employed to label microorganisms.[12] Considerable research has also been published focusing on the use of magnetic particles for water treatment.[13,14]

* Corresponding author: Prof. Judy S. Riffle. Phone: 540-231-8214. Fax: 540-231-8517. E-mail: judyriffle@aol.com.
[†] Virginia Polytechnic Institute and State University.
[‡] School of Physics, The University of Western Australia.
[§] Center for Microscopy and Microanalysis, The University of Western Australia.

(1) Berkovski, B. *Magnetic Fluids and Applications Handbook*; Begell House, Inc.: New York, 1996.
(2) Hess, P.; Parker, P. *J. Appl. Polym. Sci.* **1966**, *10* (12), 1915.
(3) Rosensweig, R. E. *Ferrohydrodynamics*; Cambridge University Press: Cambridge, MA, 1985.
(4) Smith, T.; Wychick, D. *J. Phys. Chem.* **1980**, *84*, 1621.
(5) Papirer, E.; Horny, P. *J. Colloid Interface Sci.* **1983**, *94*, 207.
(6) Fertman, V. *Magnetic Fluids Guidebook: Properties and Applications*; Hemisphere Publishing Corp.: New York, 1990; p 858.
(7) Yu, J.; Hafeli, U.; Li, Y.; Failing, S.; Leakakos, T.; Tapolsky, G. *Proc. 4th International Conference on the Scientific and Clinical Applications of Magnetic Carriers*, Tallahassee, FL, 2002; Cleveland Clinic Foundation: Cleveland, 2002; p 16.
(8) Bulte, J.; Douglas, T.; Failing, S.; Leakakos, T.; Tapolsky, G. *Proc. 4th International Conference on the Scientific and Clinical Applications of Magnetic Carriers*, Tallahassee, FL, 2002; Cleveland Clinic Foundation: Cleveland, 2002; p 26.
(9) Plank, C.; Scherer, F.; Schillinger, U.; Anton, M.; Bergemann, C. *Proc. 4th International Conference on the Scientific and Clinical Applications of Magnetic Carriers*, Tallahassee, FL, 2002; Cleveland Clinic Foundation: Cleveland, 2002; p 93.
(10) Hofer, K. *Proc. 4th International Conference on the Scientific and Clinical Applications of Magnetic Carriers*, Tallahassee, FL, 2002; Cleveland Clinic Foundation: Cleveland, 2002; p 78.
(11) Cremer, A.; Reinhard, C.; Muller, S.; Gunther, G.; Kohler, M.; Koster, M.; Heckel, N.; Bierver, C.; Johnston, I.; Merkel, D.; Nolle, V.; Miltenyi, S. *Proc. 4th International Conference on the Scientific and Clinical Applications of Magnetic Carriers*, Tallahassee, FL, 2002; Cleveland Clinic Foundation: Cleveland, 2002; p 73.
(12) Puntes, V.; Parak, W.; Alivisatos, A. *Proc. 4th International Conference on the Scientific and Clinical Applications of Magnetic Carriers*, Tallahassee, FL, 2002; Cleveland Clinic Foundation: Cleveland, 2002; p 143.

10.1021/cm0482028 CCC: $30.25
Published on Web 09/21/2005

Iron oxides such as magnetite (Fe_3O_4) and maghemite (γ-Fe_2O_3), as well as the transition metals Co, Ni, and Fe, have the capacity to generate magnetic materials.[1] The vast majority of ferrofluid and magnetic particle research for biotechnological applications focuses on iron oxides because of their oxidative stability and biological compatibility. Magnetic materials consisting of cobalt metal nanoparticles, however, have the potential for three to four times the magnetic response of the iron oxides. Nonetheless, the development of cobalt particles for all applications is limited by the fact that cobalt nanoparticles oxidize slowly in air, forming antiferromagnetic cobalt oxides. Consequently, methodologies that afford protective coatings to prevent oxidation of these particles are desirable before they may be considered for long-term use under ambient conditions.

Herein we report the formation of oxidatively stable, cobalt−graphitic nanoparticles with high saturation magnetizations via elevated heat treatments of cobalt nanoparticles encapsulated with poly(styrene-*b*-4-vinylphenoxyphthalonitrile). These nanoparticles were synthesized by thermolysis of dicobalt octacarbonyl in solutions of toluene containing poly(styrene-*b*-4-vinylphenoxyphthalonitrile). The nanoparticles were subsequently heated under inert conditions to afford a protective carbonaceous coating.

Experimental Section

Materials. Tetrahydrofuran (THF; 99.5%, E.M. Sciences) was dried over calcium hydride overnight and then refluxed over sodium in the presence of benzophenone until the solution was a deep purple. The THF was distilled just prior to use. Styrene (Aldrich, 99%) was stirred over calcium hydride for 24 h and distilled prior to use. Chemfirst, Inc., kindly donated 4-acetoxystyrene, which was used as received. Potassium hydroxide, diethyl ether, imidazole, *N*,*N*-dimethylformamide (DMF), magnesium sulfate, *n*-butyllithium (2.0 M in *n*-hexane), and *tert*-butyldimethylchlorosilane were purchased from Aldrich and used as received. Dicobalt octacarbonyl (Alfa Aesar) was transferred to sealed glass vials in a drybox and stored at −10 °C until used. Toluene (Aldrich, 99%) was stirred over calcium hydride and distilled prior to use. 1-Methyl-2-pyrrolidinone (NMP) was purchased from Fisher Scientific, dried over calcium hydride, and distilled into a round-bottom flask containing activated molecular sieves. 4-Nitrophthalonitrile was synthesized using the procedure of Sumner.[15]

Synthesis of 4-Vinylphenol. Potassium hydroxide (44 g, 0.78 mol) and 500 mL of deionized water were charged to a 1000-mL, single-neck round-bottom flask. The solution was cooled in an ice bath to 0 °C, and 50 mL (0.33 mol) of 4-acetoxystyrene was injected with rapid stirring to afford a yellow slurry. The reaction mixture was maintained at 0 °C for 5 h, and the medium became transparent during this period. Approximately 30 mL of HCl (11.97 M) was added dropwise to precipitate the product. The monomer was collected using vacuum filtration, washed with deionized water, and dried under vacuum at room temperature for 24 h. Approximately 90% yield was obtained.

Synthesis of *tert*-Butyldimethylsilyloxystyrene. *tert*-Butyldimethylsilyloxystyrene was synthesized by the method of Hirao et al.[16] A flame-dried, 250-mL, single-neck, round-bottom flask, equipped with a magnetic stir bar, was charged with 4-vinylphenol (20 g, 0.17 mol) and imidazole (28.4 g, 0.42 mol) and capped with a septum under argon. Approximately 200 mL of DMF was added via syringe, and the reaction mixture was cooled to 0 °C. A solution of *tert*-butyldimethylchlorosilane (31.3 g, 0.21 mol) in DMF (40 mL) was added dropwise over ∼30 min. The mixture was warmed to room temperature and reacted for 12 h. Approximately 100 mL of an aqueous 10 M NaOH solution was added, followed by 200 mL of diethyl ether to extract *tert*-butyldimethylsilyloxystyrene. The layer containing the product in diethyl ether was isolated using a separatory funnel and washed eight times with aqueous 10 M NaOH solutions (200 mL each). The diethyl ether was removed under vacuum at room temperature, and *tert*-butyldimethylsilyloxystyrene was distilled under vacuum at 180 °C. Approximately 85% yield was obtained.

Synthesis of Poly(styrene-*b*-*tert*-butyldimethylsilyloxystyrene). A representative procedure for preparing a block copolymer with a 20 000 g mol^{-1} polystyrene block and a 5000 g mol^{-1} poly(*tert*-butyldimethylsilyloxystyrene) block is provided. All other poly(styrene-*b*-*tert*-butyldimethylsilyloxystyrene) block copolymers were prepared in analogous procedures, but with appropriate concentrations of the *n*-butyllithium initiator relative to monomers to control the block molecular weights. Styrene (10 g, 0.096 mol) was injected into a flame-dried, single-neck, 250-mL, round-bottom flask containing 75 mL of THF. The reaction solution was cooled to −78 °C and degassed under vacuum. The initiator *n*-butyllithium (0.25 mL of a 2.0 M solution, 0.50 mmol) was added into the vigorously stirred, cold reaction mixture via syringe. After approximately 10 min, a solution of freshly distilled *tert*-butyldimethylsilyloxystyrene (2.5 g, 0.011 mol) in 50 mL of THF was transferred slowly via cannula into the reaction under an argon purge. The living chain ends were terminated with degassed methanol after approximately 10 min. The copolymer was precipitated by pouring the reaction solution into a beaker of stirred methanol. The yield was quantitative (12.5 g).

Synthesis of Poly(styrene-*b*-4-vinylphenol). Deprotection of the *tert*-butyldimethylsilyl ether group was accomplished by hydrolyzing the silyl ether bond under acidic conditions. An ∼0.6 M solution of HCl in water−THF was prepared by injecting 3.0 mL of an aqueous 11.97 M HCl solution into 60 mL of THF. The poly(styrene-*b*-*tert*-butyldimethylsilyloxystyrene) copolymer (12 g, 4.8 × 10^{-4} mol) was dissolved in 60 mL of the acidic THF solution and reacted at 50 °C overnight. The copolymer was precipitated by pouring the reaction mixture into a beaker of stirred water. The product was filtered, dried under vacuum, dissolved in THF (50 mL), and reprecipitated by adding it into 500 mL of rapidly stirred hexane. The copolymer was dried in a vacuum oven for 48 h at 75 °C. The yield was quantitative (10.8 g).

Synthesis of Poly(styrene-*b*-4-vinylphenoxyphthalonitrile). Poly(styrene-*b*-4-vinylphenol) (10 g, 9.48 mequiv phenol) was dissolved in 50 mL of NMP. Anhydrous, solid potassium carbonate (3.93 g, 28.4 mmol) was added to the reaction mixture. A 20% molar excess of 4-nitrophthalonitrile (1.97 g, 11.4 mmol) with respect to phenol was charged to the reaction, and the solution was reacted at 60 °C for ∼12 h. The solution was filtered to remove salts, and the copolymer was isolated via precipitation into a beaker

(13) Pourima, B.; Pougnard, C.; Josson, C.; Baron, P. L.; Pringuez, E.; Drocourt, J.; Cabanes, P.; Legastelois, S. *Proc. 4th International Conference on the Scientific and Clinical Applications of Magnetic Carriers*, Tallahassee, FL, 2002; Cleveland Clinic Foundation: Cleveland, 2002; p 56.

(14) Gruttner, C.; Rudershausen, S.; Matthews, S.; Wang, P.; Bohmer, V.; Dozol, J. F. *Proc. 4th International Conference on the Scientific and Clinical Applications of Magnetic Carriers*, Tallahassee, FL, 2002; Cleveland Clinic Foundation: Cleveland, 2002; p 59.

(15) Sumner, M. J. High Performance Materials Containing Nitrile Groups. Ph.D. Dissertation, Virginia Polytechnic Institute and State University, Blacksburg, VA, 2003.

(16) Hirao, A.; Kitamura, K.; Takenaka, K.; Nakahama, S. *Macromolecules* **1993**, *26* (19), 4995.

of stirred methanol (~500 mL). The copolymer was dried in a vacuum oven at 100 °C for 48 h. The yield of copolymer was nearly quantitative (11 g).

Cobalt Ferrofluid Formation. A three-neck, 250-mL, round-bottom flask equipped with a condenser, mechanical stirrer, and a septum-capped neck was flame-dried under argon. Approximately 50 mL of toluene was injected into the flask. A poly(styrene-*b*-4-vinylphenoxyphthalonitrile) copolymer (0.50 g, 1.42×10^{-5} mol, 0.423 mequiv phthalonitrile) was added quickly and dissolved. The reaction medium was deoxygenated by purging argon through the solution for 2 h. One gram of dicobalt octacarbonyl (2.93 mmol) was quickly charged to the flask, and the reaction was refluxed at 110 °C for 5 h. The solution was cooled to room temperature, transferred to a flame-dried, septum-capped, 100-mL, round-bottom flask via cannula, and stored under argon.

Pyrolysis of Cobalt−Copolymer Complexes. Toluene was removed from the ferrofluids under vacuum at 100 °C for ~24 h. Approximately 1 g of the cobalt−copolymer complex was placed in a ceramic boat and positioned in the center of a quartz tube in a tube furnace. The material was heated under an argon purge at 500 °C for 4 h, cooled to room temperature, then heated at 700 °C for 4 h, and cooled to room temperature.

Grinding of Pyrolyzed Cobalt−Copolymer Complexes. Pyrolyzed cobalt−copolymer complexes were ground in a Puluerisette intensive ball mill. Approximately 0.25 g of the pyrolyzed material was placed in a 25-mL grinding bowl equipped with seven steel grinding balls (25 mm). Toluene (5 mL) was injected into the chamber, and the material was ground for 2 h at 700 rpm. The resultant slurry was poured into a single-neck, 50-mL, round-bottom flask and dried under vacuum at 150 °C for 24 h.

^{1}H NMR Spectroscopy. A Varian Unity 400 MHz NMR spectrometer was used to collect ^{1}H NMR spectra of the reagents, monomers, and copolymers. Proton NMR was also employed to confirm the conversion of vinyl functional groups during the anionic polymerization reactions. The instrument was operated at a frequency of 399.954 MHz, with a recycle delay of 1 s, an acquisition time of 3.7 s, and a 22° pulse angle.

Gel Permeation Chromatography (GPC). GPC was employed to investigate the molecular weights and molecular weight distributions of the poly(styrene-*b*-*tert*-butyldimethylsilyloxystyrene) copolymers. A Waters 2690 gel permeation chromatograph equipped with a Waters HR 0.5 + HR 2 + HR 3 + HR 4 styragel column set, an online Viscotek 100 differential viscometric detector, and a Viscotek laser refractometer was used for chromatographic analysis. Chloroform was employed as the mobile phase at 25 °C and a flow rate of 1.0 mL min^{-1}. Polystyrene standards were used to construct a calibration plot in which the product of intrinsic viscosity and molecular weight was plotted as a function of elution volume. The molecular weights of the samples were determined using the universal calibration parameter.

Infrared Spectroscopy. A Nicolet Impact 400 Fourier tranform infrared (FTIR) spectrometer was used to verify the presence of hydroxyl and phthalonitrile functional groups in poly(styrene-*b*-4-vinylphenol) and poly(styrene-*b*-4-vinylphenoxyphthalonitrile). All spectra were acquired on thin films which had been solution cast onto KBr disks.

Transmission Electron Microscopy (TEM). A Philips 420T TEM run at 100 kV was used to obtain electron micrographs of the dried cobalt ferrofluids. The TEM samples were prepared by casting a few drops of the magnetic fluid, which had been diluted with toluene until it was the color of "weak tea", onto a carbon-coated copper grid and allowing the toluene to evaporate. High-resolution transmission electron microscopy (HRTEM) was conducted on a dried pyrolyzed sample using a JEOL 3000F field-emission gun transmission electron microscope operated at 300 kV. The samples were prepared by embedding them in a resin and microtoming ~100 nm slices. The slices were then placed on a carbon-coated copper grid for analysis. Selected area electron diffraction (SAED), nanobeam electron diffraction (NBD), and Fourier transform analyses of the TEM images were performed to investigate the nature of particle crystallinity.

Scanning Electron Microscopy (SEM). A LEO 1550 field-emission scanning electron microscope was employed to analyze the surface morphologies of the pyrolyzed complexes. A 5 kV electron beam accelerating voltage was used with an in-lens detector.

Thermogravimetric Analysis (TGA). A TA Instruments Q0500 thermogravimetric analyzer was used to investigate the degradation behavior of the poly(styrene-*b*-4-vinylphenoxyphthalonitrile) copolymers under inert conditions. The samples (8−10 mg) were heated from 30 to 700 °C at a ramp rate of 10 °C/min in platinum pans under a nitrogen atmosphere. Sample weight loss was monitored as a function of temperature, and the char yields afforded at 700 °C were recorded for each sample.

Magnetometry. A Lakeshore 7300 Series vibrating sample magnetometer was employed for magnetization measurements of the cobalt ferrofluids and pyrolyzed particles. All measurements were carried out in applied fields from +8000 to −8000 Oe and a sensitivity setting of 0.1 emu. A Quantum Design magnetic properties measurement system (MPMS-7) using a superconducting quantum interference device (SQUID) sensor was used to make measurements of cobalt specific magnetization (σ) in applied magnetic fields (H) over the range from −70 000 to +70 000 Oe at room temperature and 5 K. Low-temperature measurements were made both after cooling the sample in zero applied field and in an applied field of 70 000 Oe. These measurements were used to investigate the presence of any (1) paramagnetic cobalt species and (2) cobalt oxide on the surfaces of metallic cobalt particles.

Elemental Analysis of Cobalt Concentrations. Elemental analyses for cobalt were performed by the Marine and Freshwater Laboratory at Murdoch University, Western Australia. Elemental analyses were conducted on two fractions of the same sample. The first sample of pyrolyzed cobalt−graphitic complexes (D1) was acid-digested by treating the sample with 1:1 HNO_3/H_2SO_4 (35 mL total) at 70−100 °C for 4 days. The second sample of pyrolyzed cobalt−graphitic complexes (D2) was acid-digested by treating the sample with 1:1 HNO_3/H_2SO_4 (35 mL total) at 70−100 °C for 9 days and then adding concentrated H_2SO_4 (5 mL) and continuing the digestion for another 4 days. These solutions were analyzed by inductively coupled plasma atomic emission spectroscopy (ICP-AES) to determine cobalt concentrations.

Electron Diffraction. SAED was employed to study the crystallinities of the pre-pyrolyzed and pyrolyzed samples. In addition, NBD was used to probe the crystal structure of the pyrolyzed sample (1.9 nm beam diameter). All electron diffraction measurements were conducted using a JEOL 3000F field-emission transmission electron microscope operated at 300 kV.

Results and Discussion

There have been numerous reports of forming metal nanoparticles by reacting organometallic precursors in solutions of copolymer aggregates.[2,17−24] These have included solutions of block copolymers,[17,22] statistical (random) copolymers,[2] step-growth polymers,[2] and surfactants.[5] As clearly underscored in the pioneering work of Hess and Parker in the mid 1960s, the coordinating species in all systems have consisted of pendent moieties that were more

polar than the solvent system employed for particle formation.[2] The hypothesis is that the metal precursors coordinate with an electron-rich segment of the copolymer and, upon heating, the copolymers displace the precursor ligands (e.g., carbon monoxide) to afford metal nanoparticles encased in a copolymer sheath. It is reasoned that this could result from diffusion of the metal precursor into the core of a copolymer micelle where coordination and then reaction take place. On the other hand, the precursor might first coordinate with nonaggregated copolymers in solution, and the metal might serve as the species which causes the aggregates to form.

This paper describes the design and synthesis of poly(styrene-*b*-4-vinylphenoxyphthalonitrile) diblock copolymer templates prepared in living anionic polymerizations, so that the block lengths are well-controlled. Toluene solutions of these copolymers and dicobalt octacarbonyl were utilized to generate discrete cobalt nanoparticles. The polystyrene block of the copolymers is solvated well by toluene (the dispersion solvent), whereas the polyvinylphenoxyphthalonitrile block is only sparingly soluble in toluene. The nitriles apparently coordinate with dicobalt octacarbonyl so that the polyvinylphenoxyphthalonitrile serves as the so-called anchor block, and the polystyrene tail blocks protrude out into the solvent to form a sterically stabilizing corona for the complexes in the dispersions. Aromatic polymer networks containing phthalonitriles are well-known to form high levels of residual char upon pyrolysis,[25−27] and this was a major motivation for investigating copolymers containing such moieties in this research. It was reasoned that polymers with phthalonitrile groups might afford a graphitic-like coating for the cobalt nanoparticles when the complexes were heated to elevated temperatures.

Synthesis of Diblock Copolymer Dispersion Stabilizers and Formation of Cobalt Nanoparticle Ferrofluids. Poly(styrene-*b*-*tert*-butyldimethylsilyloxystyrene) copolymers were synthesized in living anionic polymerizations via sequential polymerization of styrene followed by *tert*-butyldimethylsilyloxystyrene as described by Hirao et al. (Figure 1).[16] THF was employed as the reaction solvent since it readily solvates both monomers as well as high-molecular-weight poly(styrene-*b*-*tert*-butyldimethylsilyloxystyrene) copolymers. To avoid cleaving the silyl ether bond of *tert*-butyldimethylsilyloxystyrene during synthesis, the anionic polymerizations were conducted at −78 °C. Upon adding the *n*-butyllithium initiator, the reaction medium turned dark red, signifying the presence of living polystyryl anions. The solution remained dark red after adding the *tert*-butyldimethylsilyloxystyrene, again indicating the presence of active styrenic species.

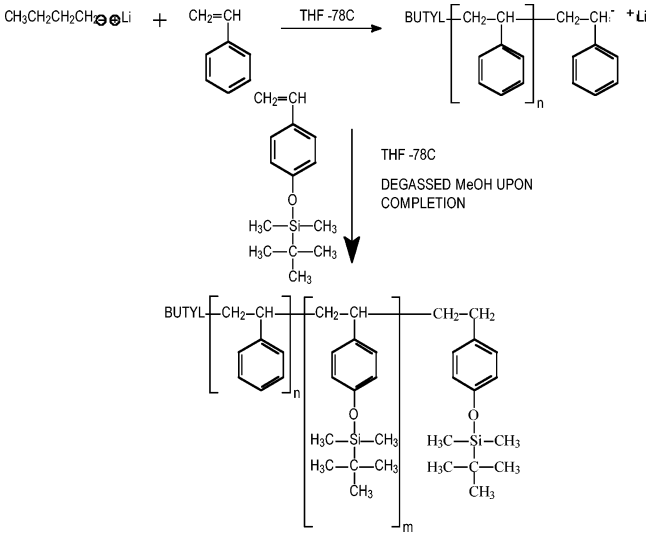

Figure 1. Synthesis of poly(styrene-*b*-*tert*-butyldimethylsilyloxystyrene).

Table 1. Molecular Weights of Poly(styrene-*b*-*tert*-butyldimethylsilyloxystyrene) Copolymers

targeted styrene block M_n	targeted protected phenol block M_n	M_n (GPC)	PDI
20 000	5 000	25 000	1.05
30 000	5 000	35 900	<1.03
40 000	10 000	51 600	<1.03
50 000	20 000	80 000	1.04
50 000	10 000	58 400	1.06
75 000	10 000	80 000	1.08

Proton NMR was utilized to monitor the progress of the copolymerizations by observing the disappearance of the vinyl protons of both monomers ($\delta = 5.2$, 5.6, and 6.7 ppm). An aliquot of the reaction medium taken immediately after adding the *n*-butyllithium indicated that quantitative conversion of the vinyl protons had already occurred. Similarly, ^{1}H NMR of the reaction just after adding *tert*-butyldimethylsilyloxystyrene also indicated that quantitative conversion of the monomer occurred within seconds. The rapid reaction rates were anticipated because THF affords solvent-separated ion pairs and highly reactive chain centers.

A series of poly(styrene-*b*-*tert*-butyldimethylsilyloxystyrene) copolymers with systematically varied molecular weights were synthesized (Table 1). GPC of the copolymers revealed narrow, monomodal peaks with polydispersities reflective of living anionic polymerizations. In addition, ^{1}H NMR of the isolated copolymers exhibited proton resonances indicative of the polystyrene and poly(*tert*-butyldimethylsilyloxystyrene) blocks (Figure 2).

The silyl ether bonds of poly(styrene-*b*-*tert*-butyldimethylsilyloxystyrene) were readily cleaved in an acid-promoted deprotection reaction in THF. Proton NMR of the block copolymers after acidic treatment indicated that quantitative deprotection of the poly(*tert*-butyldimethylsilyloxystyrene) block was achieved. The *tert*-butylsilyl and dimethylsilyl proton sets at 1.0 and 0.2 ppm were absent from the spectra of the isolated copolymers. Moreover, the hydroxyl group

(17) Sastri, S. B.; Armistead, J. P.; Keller, T. M.; Sorathia, U. *Polym. Compos.* **1997**, *18*, 48.
(18) Sastri, S. B.; Keller, T. M. *J. Appl. Polym. Sci.* **1998**, *36*, 1885.
(19) Sastri, S. B.; Keller, T. M. *J. Appl. Polym. Sci.* **1999**, *37*, 2105.
(20) Sumner, M. J.; Sankarapandian, M.; McGrath, J. E.; Riffle, J. S. *Polymer* **2002**, *43*, 5069.
(21) Sumner, M. J.; Sankarapandian, M.; McGrath, J. E.; Riffle, J. S.; Sorathia, U. *International SAMPE Technical Conference*; SAMPE: Covina, CA, 2001; Vol. 33, p 1509.
(22) Tannenbaum, R. *Inorg. Chim. Acta* **1997**, *227*, 233.
(23) Nogues, J.; Schuller, I. K. *J. Magn. Magn. Mater.* **1999**, *192*, 203.
(24) Connolly, J.; St. Pierre, T. G.; Rutnakornpituk, M.; Riffle, J. S. *Eur. Cells Mater.* **2002**, *3*, 106.
(25) Connolly, J.; St. Pierre, T. G.; Rutnakornpituk, M.; Riffle, J. S. *J. Phys. D: Appl. Phys.* **2004**, *37*, 2475.
(26) Ruisheng, X.; Zengmin, S. *Carbon* **2003**, *41*, 1851.
(27) Terrones, M.; Grobert, N.; Olivares, J.; Zhang, J. P.; Terrones, H.; Kordatos, K.; Hsu, W. K.; Hare, J. P.; Townsend, P. D.; Prassides, K.; Cheatham, A. K.; Kroto, H. W.; Walton, D. R. M. *Nature* **1997**, *388*, 52.

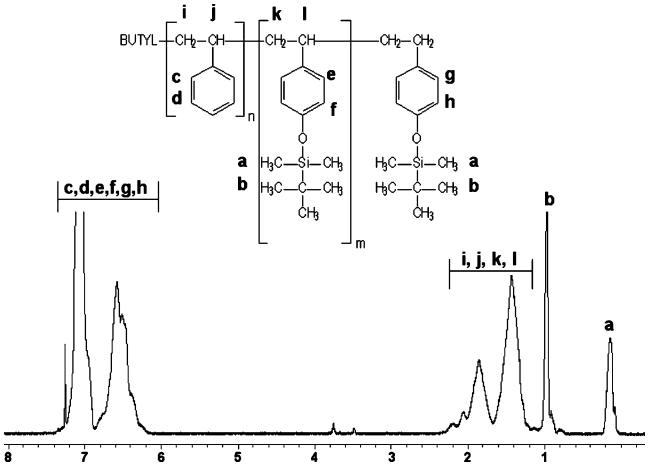

Figure 2. ^{1}H NMR of poly(styrene-*b*-*tert*-butyldimethylsilyloxystyrene). The *tert*-butylsilyl and dimethylsilyl protons of the protected phenol block resonate at 1.0 and 0.2 ppm, respectively.

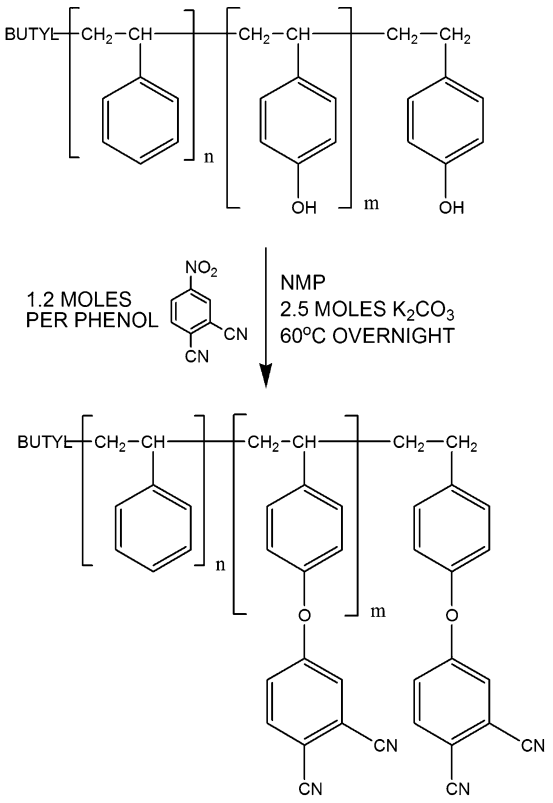

Figure 3. Synthesis of poly(styrene-*b*-4-vinylphenoxyphthalonitrile).

of poly(styrene-*b*-4-vinylphenol) was observed in the FTIR spectra of the deprotected copolymers at ~3500 cm^{-1}.

Poly(styrene-*b*-4-vinylphenoxyphthalonitrile) was synthesized by chemically modifying poly(styrene-*b*-4-vinylphenol) with 4-nitrophthalonitrile via a nucleophilic aromatic substitution reaction under basic conditions in NMP (Figure 3). Proton NMR of the isolated copolymers indicated that the chemical modification reaction was quantitative (Figure 4). The integral ratios of the peaks due to the aromatic protons ortho to the phthalonitrile groups at 7.75 ppm to the remaining, overlapping aromatic proton resonances at 6.3−7.2 ppm were equivalent to the theoretical ratios for all of the phthalonitrile-containing block copolymers. FTIR also qualitatively confirmed chemical modification with 4-nitrophthalonitrile. The characteristic stretch of the nitrile moieties

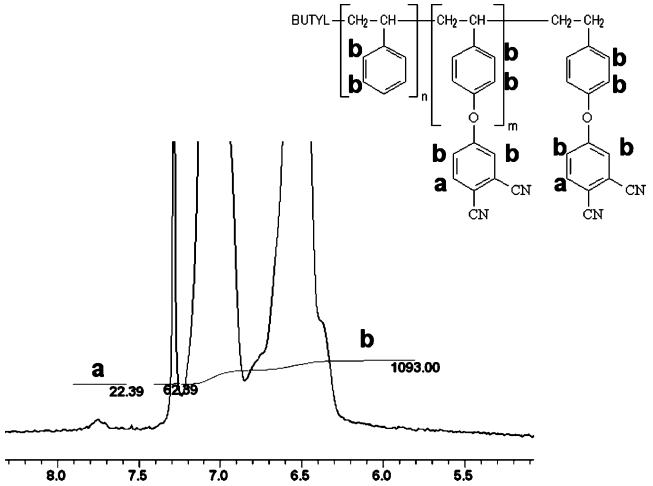

Figure 4. ^{1}H NMR of the aromatic region of a poly(styrene-*b*-4-vinylphenoxyphthalonitrile) copolymer. The integration ratio of the aromatic proton set ortho to the phthalonitrile group (22.4) to the overlapping aromatic proton sets (1093.0) is nearly equivalent to the theoretical integral ratio (22/2093) for a poly(styrene-*b*-4-vinylphenoxyphthalonitrile) copolymer.

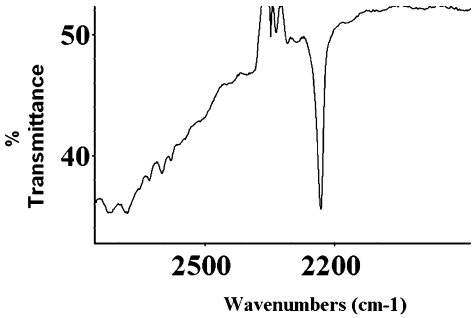

Figure 5. FTIR spectrum of poly(styrene-*b*-4-vinylphenoxyphthalonitrile). The nitrile stretch is present at ~2230 cm^{-1}.

was observed in the poly(styrene-*b*-4-vinylphenoxyphthalonitrile) copolymers at ~2230 cm^{-1} (Figure 5).

Dynamic weight loss profiles of a series of the diblock copolymers were evaluated by heating them in a TGA instrument at temperatures up to 700 °C under a nitrogen atmosphere to determine whether the phthalonitrile groups in these materials led to significant residual carbonaceous char. An abrupt weight loss was observed for all of the diblock copolymers at ~400 °C, and the residue after that drop was retained by these materials up to the end of the experiments (700 °C). A copolymer with a 30 000 g mol^{-1} polystyrene block and a 5256 g mol^{-1} polyvinylphenoxyphthalonitrile block retained about 20 wt % of carbonaceous residue, whereas a copolymer with a 75 000 g mol^{-1} polystyrene block and a 10 512 g mol^{-1} polyvinylphenoxyphthalonitrile block retained approximately 50% of its original weight. Such high residues after the elevated heat treatments were encouraging because it was reasoned that these residues might result in robust carbonaceous coatings for the cobalt nanoparticles. The polymeric nature of these copolymers may also be important for obtaining char residues with sufficient mechanical integrity to withstand subsequent intensive ball milling without exposing the cobalt surfaces.

A block copolymer with a 5256 g mol^{-1} polyvinylphenoxyphthalonitrile block molecular weight was utilized for investigating the formation of protective carbonaceous coatings around the cobalt nanoparticles. It should be noted,

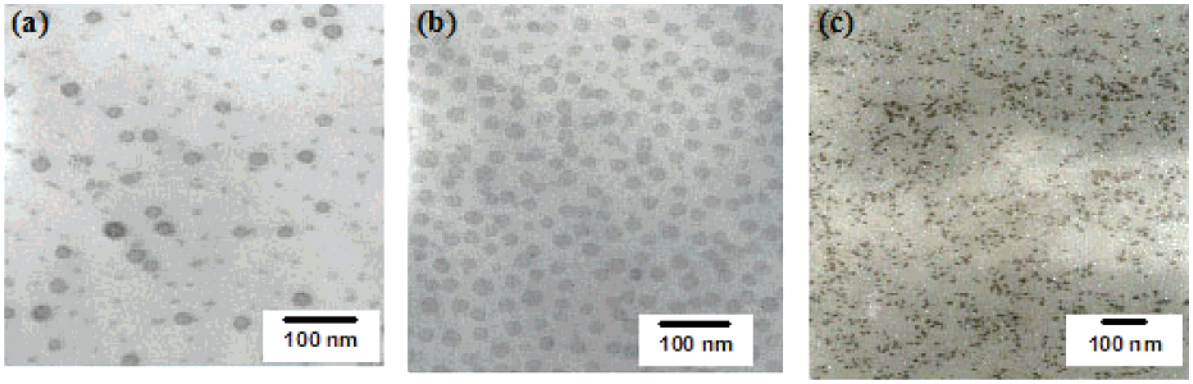

Figure 6. (a) TEM micrograph of a reaction solution containing 1 g of dicobalt octacarbonyl and 0.5 g of a 28 000 g mol^{-1} poly(styrene-*b*-4-vinylphenoxyphthalonitrile) copolymer in toluene at room temperature immediately after mixing. (b) Within 15 min of heating at toluene reflux. (c) After 4 h at toluene reflux.

however, that all poly(styrene-*b*-4-vinylphenoxyphthalonitrile) copolymers derived from the template copolymers listed in Table 1 were successfully employed to form stable suspensions of cobalt nanoparticles. Cobalt ferrofluids were prepared by thermally reacting dicobalt octacarbonyl in concentrated toluene solutions of poly(styrene-*b*-4-vinylphenoxyphthalonitrile). FTIR spectroscopy was used to monitor the thermolysis of $Co_2(CO)_8$ to form metallic cobalt. FTIR of the reaction mixture immediately after adding the $Co_2(CO)_8$ revealed carbonyl stretches at 2030, 2065, and 1858 cm^{-1}. Aliquots of the reaction medium immediately after heating to 110 °C revealed the characteristic absorption bands of $Co_4(CO)_{12}$ at 2058 and 1867 cm^{-1} as reported previously by Tannenbaum.[22] After refluxing the reaction solution at 110 °C for 5 h, the characteristic carbonyl stretches of $Co_4(CO)_{12}$ were dramatically reduced. However, residual carbonyl stretches were still observed at 2058 and 1867 cm^{-1}.

Aliquots of the reaction solutions or dispersions were solvent-cast onto carbon-coated copper TEM grids to observe the nature of the aggregates during synthesis (Figure 6). Immediately after adding dicobalt octacarbonyl into the copolymer solution (left side of Figure 6), cobalt aggregates as well as small cobalt species which may have been free in solution at this point in the reaction were visible. Soon after reaching the toluene reflux temperature (middle of Figure 6), uniform cobalt aggregates were observed, probably encased in micelles of the block copolymer. TEM of solvent-cast ferrofluids after 4 h of reaction indicated that the precursor aggregates had densified and become smaller (right side of Figure 6). Well-dispersed, spherical cobalt nanoparticles ∼8−10 nm in diameter had formed, most likely encased in copolymer sheaths. Although it should be recognized that this analysis does not provide information on the mechanism of aggregate formation, it does demonstrate that the cobalt particles form within the small copolymer aggregates. This perhaps also accounts for the relatively narrow particle size distribution and the fact that each cobalt nanoparticle seems to be discrete.

Magnetic susceptometry measurements (using a SQUID-based sensor) were conducted on a dried pre-pyrolyzed sample that had been exposed to ambient conditions for 3 months. Room-temperature measurements indicated a saturation magnetization of 30 emu g^{-1} material (80 emu g^{-1} Co). A magnetic remanence of 7 emu g^{-1} material (19 emu g^{-1} Co) and a coercivity of 410 Oe were observed, indicating that at least part of the sample was magnetically blocked at room temperature. Low temperature σ versus H measurements indicated an asymmetric shift in the field-cooled hysteresis loop with respect to the zero field-cooled hysteresis loop (Figure 7). This loop shift is indicative of the coupling of an antiferromagnetic cobalt oxide layer with a ferromagnetic cobalt core.[23] We have observed that the cobalt−copolymer complexes (without a pyrolysis step) undergo a slow loss in saturation magnetization. This evidence supports the explanation for the decline in saturation magnetization over time being at least partially attributed to cobalt oxidation. In addition, the cobalt specific magnetization (σ) showed a continuous increase with field at high fields and low temperature. However, at room temperature σ almost saturated at high fields. These observations are consistent with the presence of paramagnetic species within the sample. This paramagnetic component is possibly due to residual cobalt species that have not been incorporated into the cobalt nanocrystals.[24,25]

Preparation and Characterization of Cobalt Nanoparticles Encased in Protective Graphitic-like Coatings. The complexes of cobalt metal nanoparticles coated with poly(styrene-*b*-4-vinylphenoxyphthalonitrile) were heated at elevated temperatures to convert the copolymers to carbonaceous coatings for protecting the metal against oxidation. The ferrofluid solvent was removed under vacuum, then the complexes were pyrolyzed at 400−700 °C in a tube furnace under an argon purge. This produced ensembles of particles adhered together by the pyrolyzed carbonaceous matrix. As expected based on the weight loss profiles of the copolymers (from TGA), some weight was lost in these processes. Thus, it was anticipated that the specific saturation magnetizations of the complexes would increase upon pyrolysis. Surprisingly, however, the increase in magnetization after treating the complexes at 600−700 °C was significantly greater than expected, and this could not be attributed merely to weight loss (Figure 8).

Transmission electron micrographs of microtomed thin sections of the complexes heated at 700 °C showed both 8−10 nm particles (the original size), together with a substantial portion of irregularly shaped, 50−150 nm agglomerates within the carbonaceous matrix. The micrographs suggest that some cobalt particle sintering had taken place

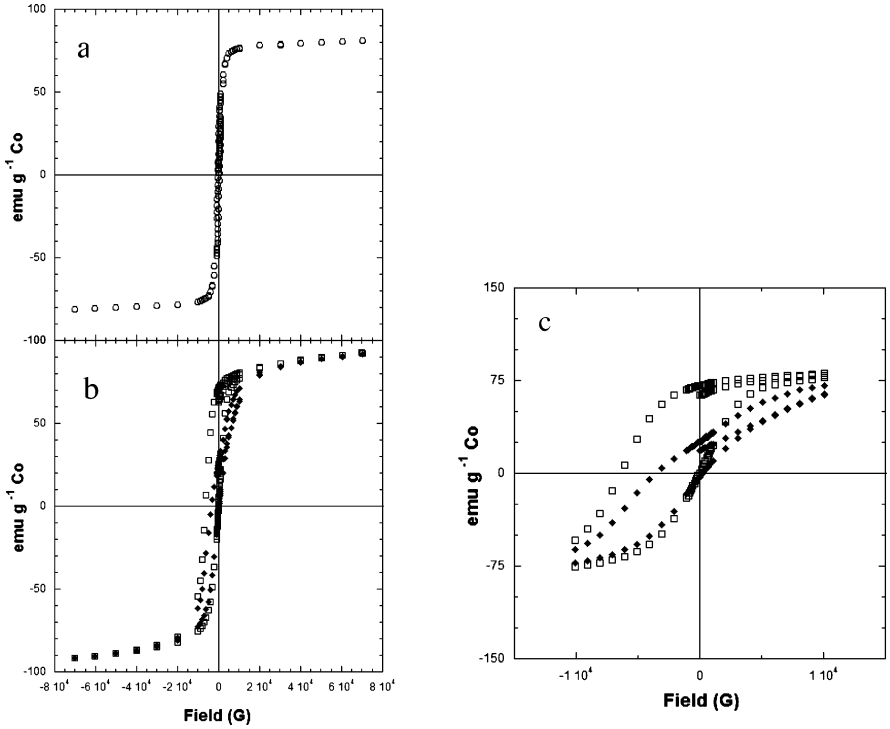

Figure 7. σ versus H measurements conducted at (a) 300 and (b) 5 K (zero-field-cooled hysteresis loop, ◆; field-cooled hysteresis loop, □) on pre-pyrolyzed cobalt−polymer complexes that had been aged under ambient conditions for 3 months. (c) Enlarged regions around the origin for 5 K hysteresis loops showing the asymmetric field-cooled hysteresis loop shift.

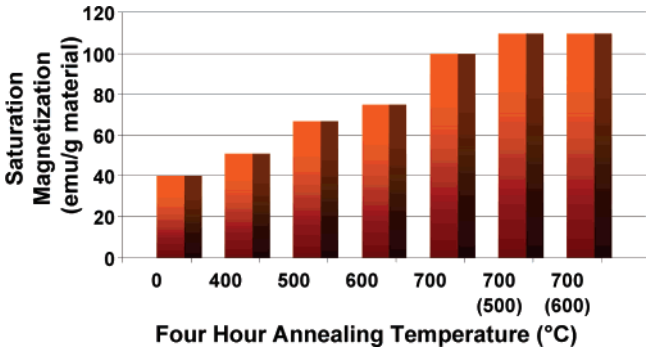

Figure 8. Specific saturation magnetizations of cobalt−copolymer complexes after heating for 4 h at the designated temperatures. The two complexes on the right were first heated for 4 h at the temperatures in parentheses, cooled to room temperature, and then heated for another 4 h at 700 °C.

during the heat treatment at 700 °C. Interestingly, cross-sectional micrographs of cobalt−copolymer complexes that were pyrolyzed at 500 °C for 4 h, then at 700 °C for 4 h, revealed a majority of 8−10 nm particles together with some of the 50−150 nm agglomerates, and the particles seemed to have more spherical character as compared to those heated only at 700 °C (Figure 9). The reasons for the somewhat different appearances of the particles subjected to different heat treatments will require significant further study. However, it is reasoned that the matrix should undergo weight loss with cross-linking at 500 °C and that this may somewhat inhibit cobalt particle sintering during the 700 °C step.

The high saturation magnetizations of the cobalt nanoparticle complexes have been retained after aging under ambient conditions for over 1 year (Figure 10). Because cobalt oxides are antiferromagnetic, retention of the high magnetizations demonstrates the oxidative stability of these

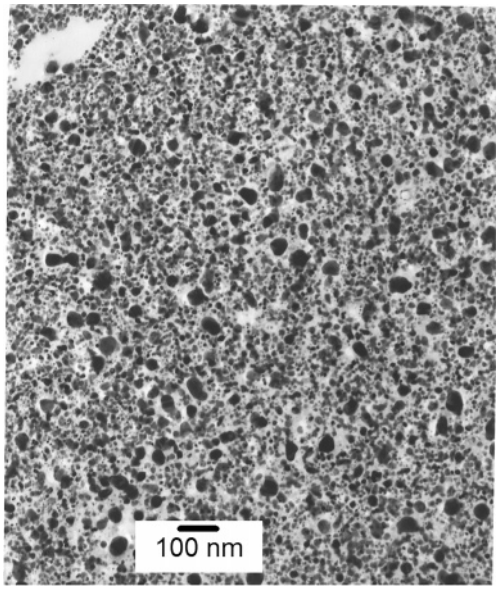

Figure 9. TEM micrograph of a thin section of cobalt nanoparticles coated with a 25 000 g mol^{-1} poly(styrene-*b*-4-vinylphenoxyphthalonitrile) copolymer after heating to 500 °C for 4 h, cooling to room temperature, and then heating at 700 °C for 4 h.

complexes. These cobalt complexes were milled in an intensive mill at 700 rpm in an aqueous 10 M KOH solution for 2 h to obtain fine particles. The strongly basic solution was utilized because it was thought that this might etch the carbonaceous coatings sufficiently to aid in obtaining fine particles.[26] SEM of the ground particles revealed a particle size range from 10 nm to 100 μm. This milling process yields materials with a saturation magnetization of 90 emu g^{-1} material (only about a 10% loss), and this has now been aged for over 100 days without any further loss in magnetic properties (Figure 10). Thus, it is believed that the pyrolyzed

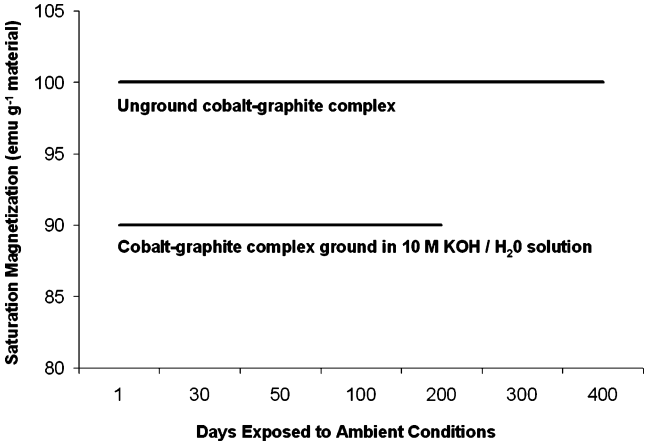

Figure 10. Specific saturation magnetization (emu g^{-1} material) as a function of days exposed to ambient conditions for cobalt particles encapsulated with a poly(styrene-*b*-4-vinylphenoxyphthalonitrile) copolymer (5256 g mol^{-1} polyvinylphenoxyphthalonitrile block molecular weight and 30 000 g mol^{-1} polystyrene block molecular weight) pyrolyzed at 700 °C for 4 h under an argon purge (top) and the same material after grinding at 700 rpm for 2 h in an aqueous 10 M KOH solution (bottom).

phthalonitrile-containing blocks afford a durable barrier preventing the oxidation of cobalt nanoparticles under ambient conditions.

Magnetic susceptometry measurements using a SQUID-based sensor were conducted on a pyrolyzed sample with block lengths of 50 000−10 000 g mol^{-1} poly(styrene-*b*-4-vinylphenoxyphthalonitrile) to further elucidate its magnetic properties (Figure 11). Two different values for cobalt specific saturation magnetization were obtained, associated with two different elemental analyses following two different sample digestion procedures (discussed in the following section and denoted D1 for the 4-day digestion procedure and D2 for the 13-day digestion procedure). Sample preparation for the first analysis consisted of digesting a known amount of sample in 35 mL (volume over the total digestion period) of 1:1 HNO_3/H_2SO_4. The sample was digested while heating at 70−100 °C for 4 days. The sample for the second analysis was subjected to 35 mL of 1:1 HNO_3/H_2SO_4 for 13 days with an addition of 5 mL of H_2SO_4 added on the 9th day. The sample was heated at 70−100 °C during the entire digestion process. The relatively robust nature of the protective graphitic coating is likely the cause for disagreement between the elemental analysis data. Graphite is an extremely stable and unreactive allotrope of carbon. Thus, it is reasonable that the graphitic-type coating would passivate a metallic nanoparticle, protecting it from chemical reactions (e.g., oxidation). The more rigorous digestion procedure for the second analysis resulted in higher calculated cobalt concentrations, suggesting that the protective coating can be digested over time under extreme conditions. Room-temperature measurements showed apparent saturation magnetizations of 230 emu g^{-1} of calculated Co for D1 and 172 emu g^{-1} for D2. Both the magnitude of these values and their differences indicate that the sample digestion procedure for this material is critical to the values of cobalt concentration obtained from the ICP-AES measurements. The value of 230 emu g^{-1} Co for D1 is significantly higher than the maximum cobalt specific magnetization expected based on the value for bulk cobalt and, hence, implies that the sample

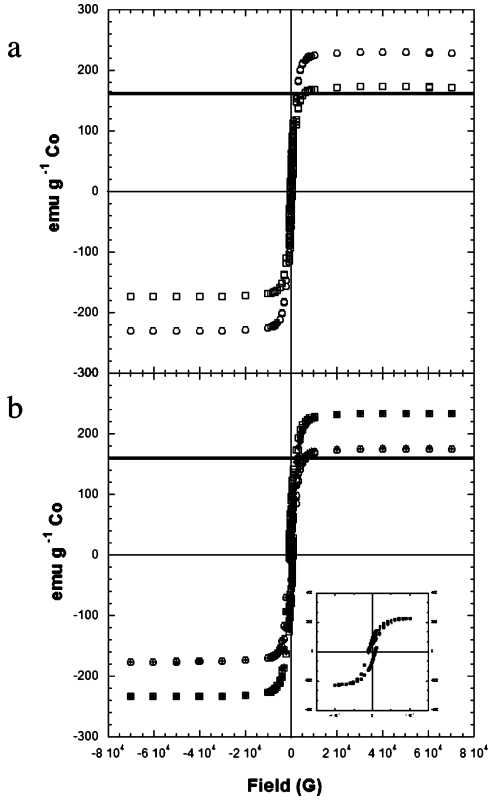

Figure 11. σ versus H measurements conducted on a cobalt−copolymer (the block lengths were 50 000 g mol^{-1} polystyrene and 10 000 g mol^{-1} polyvinylphenoxyphthalonitrile) sample that had been pyrolyzed at 700 °C at (a) 300 K (○, 4-day acid digestion, and □, 13-day acid digestion) and (b) 5 K [4-day acid digestion, zero-field-cooled (□), field-cooled (■); 13-day acid digestion, zero-field-cooled (○), field-cooled (+)] on a pyrolyzed sample. The inset in part b shows enlarged regions around the origin for 5 K hysteresis loops (4-day acid digestion) and shows no field-cooled hysteresis loop shift. The bold line at 160 emu g^{-1} Co indicates the theoretical maximum cobalt specific magnetization.

digestion was incomplete. The reduction in the apparent cobalt specific magnetization with increased digestion time suggests that the digestion process is very slow for this material.

Low-temperature magnetization measurements on these pyrolyzed cobalt−graphitic complexes indicate similar saturation magnetizations. Field-cooled σ versus H measurements show magnetic hysteresis with negligible field bias relative to zero-field-cooled σ versus H measurements (Figure 11b), suggesting the absence of cobalt oxide layers around the metallic cobalt particles. The long-term saturation magnetization stability (Figure 10) confirms that the pyrolyzed carbonaceous cobalt complexes are oxidatively stable. Compared to the pre-pyrolyzed sample, the cobalt specific magnetization for the pyrolyzed sample saturates at high fields in both room-temperature and low-temperature studies, indicating an absence of the paramagnetic component that was observed for the pre-pyrolyzed sample. It is believed that residual carbonyl species evolve during the pyrolysis and that this largely decreases or eliminates any paramagnetic species in the sample. Field-cooled and zero-field-cooled σ versus T measurements in conjunction with σ versus H measurements at room temperature suggest that both the pre-pyrolyzed and pyrolyzed samples consist of a combination of particles that are superparamagnetic and magnetically blocked at room temperature. Room-temperature hysteresis

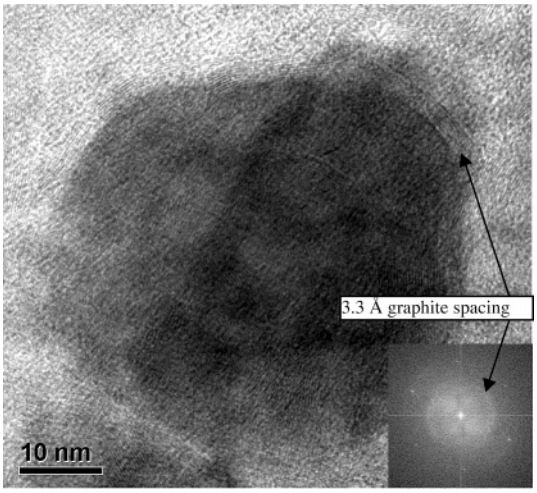

Figure 12. High-resolution transmission electron micrograph of a cobalt nanoparticle coated with graphitic layers. The inset is a Fourier transform of the image indicating the graphitic spacing and crystallinity of the particle.

loop measurements show that both samples exhibit magnetic remanence and coercivity (pre-pyrolyzed sample, $H_c = 410$ Oe, $M_r = 19$ emu g^{-1} Co; pyrolyzed sample, $H_c = 416$ Oe, $M_r = 34$ emu g^{-1} Co). TEM was employed to study the structure and morphology of the pyrolyzed cobalt−polymer composites. The particle size distribution was quite broad and suggested that some sintering had taken place during the heat treatment. The diffraction contrast across the large particles was continuous, indicating that some small particles had indeed fused. The heat treatments resulted in complex crystalline particles, which have been difficult to classify uniquely as any of the known phases of cobalt (fcc, hcp, or epsilon). Elemental mapping using a Gatan image filter (GIF) was used to confirm the elemental identity of the particles (images not shown) before conducting HRTEM. The sample consisted of highly crystalline particles, which facilitated the imaging of lattice fringes and "graphitic" coatings (Figure 12). The Fourier transform of the image in Figure 12 (inset) indicates that the particles are strongly crystalline. The measured 3.3 Å spacing for the inner ring of the Fourier transform is consistent with literature values for the interlayer spacing of graphite (3.4 Å).[27] The "graphitic" sheets follow the contour of the particle and may possibly act as the barrier that protects the particles against oxidation. SAED patterns were difficult to interpret owing to the complex nature of the crystalline cobalt particles, so NBD, with a focused 1.9-nm diameter probe, was used to obtain zone-axis diffraction patterns from individual crystal grains. The diffraction information from SAED and NBD, in conjunction with Fourier transforms of several crystalline particle images, suggest that the sample is comprised of a mixture of cobalt phases (fcc, hcp, epsilon, and perhaps others). However, further study is required to ascertain the true crystallographic nature of the particles.

Conclusions

Poly(styrene-*b*-4-vinylphenoxyphthalonitrile) copolymers have been employed to form stable dispersions of magnetic cobalt nanoparticles ~8−10 nm in diameter. These particles were converted to oxidatively stable entities by pyrolysis in inert atmospheres. Low-temperature magnetic susceptometry measurements confirmed the absence of cobalt oxide in the pyrolyzed materials. Protective carbonaceous coatings resulted from the pyrolysis, as evidenced by TEM analysis. These graphitic-type coatings are believed to be the barrier against oxidation of the pyrolyzed cobalt−polymer complexes. The pyrolyzed complexes exhibited minimal magnetic hysteresis and have retained their high saturation magnetizations (~95−100 emu g^{-1}) under ambient conditions for over 1 year. Future work will be devoted to understanding the crystalline nature of the cobalt within the pyrolyzed complexes and controlling particle size during the pyrolysis procedure. Methods for "re-functionalizing" the graphitic-type coatings following the pyrolysis and ball milling will also be important for any biomedical applications.

Acknowledgment. The authors of this paper graciously acknowledge the support of NSF under Contract No. DMR-0312046, DARPA-AFOSR (Contract Nos. F49620-02-1-0408 and F49620-03-1-0332) and OMNOVA Solutions for funding. M.A.Z. thanks the Australian-American Fulbright Commission for a Fulbright Postgraduate Fellowship to conduct research in Australia.

CM0482028